

**$^{139}\text{La}$  NMR investigation of the charge and spin order in a  $\text{La}_{1.885}\text{Sr}_{0.115}\text{CuO}_4$  single crystal**

A. Arsenault and S. K. Takahashi

*Department of Physics and Astronomy, McMaster University, Hamilton, Ontario, Canada L8S4M1*


T. Imai

*Department of Physics and Astronomy, McMaster University, Hamilton, Ontario, Canada L8S4M1  
and Canadian Institute for Advanced Research, Toronto, Ontario, Canada M5G1Z8*

W. He and Y. S. Lee

*Stanford Institute for Materials and Energy Sciences, Stanford National Accelerator Laboratory, Menlo Park, California 94025, USA  
and Department of Applied Physics, Stanford University, Stanford, California 94305, USA*

M. Fujita

*Institute for Materials Research, Tohoku University, Sendai 980-8577, Japan* (Received 16 November 2017; revised manuscript received 14 January 2018; published 14 February 2018)

$^{139}\text{La}$  NMR is suited for investigations into magnetic properties of  $\text{La}_2\text{CuO}_4$ -based cuprates in the vicinity of their magnetic instabilities, owing to the modest hyperfine interactions between  $^{139}\text{La}$  nuclear spins and Cu electron spins. We report comprehensive  $^{139}\text{La}$  NMR measurements on a single-crystal sample of high- $T_c$  superconductor  $\text{La}_{1.885}\text{Sr}_{0.115}\text{CuO}_4$  in a broad temperature range across the charge and spin order transitions ( $T_{\text{charge}} \simeq 80$  K,  $T_{\text{spin}}^{\text{neutron}} \simeq T_c = 30$  K). From the high-precision measurements of the linewidth for the nuclear spin  $I_z = +1/2$  to  $-1/2$  central transition, we show that paramagnetic line broadening sets in precisely at  $T_{\text{charge}}$  due to enhanced spin correlations within the  $\text{CuO}_2$  planes. Additional paramagnetic line broadening ensues below  $\sim 35$  K, signaling that Cu spins in some segments of  $\text{CuO}_2$  planes are on the verge of three-dimensional magnetic order. A static hyperfine magnetic field arising from ordered Cu moments along the  $ab$  plane, however, begins to develop only below  $T_{\text{spin}}^{\mu\text{SR}} = 15\text{--}20$  K, where earlier muon spin rotation measurements detected Larmor precession for a small volume fraction ( $\sim 20\%$ ) of the sample. Based on the measurement of  $^{139}\text{La}$  nuclear-spin-lattice relaxation rate  $1/T_1$ , we also show that charge order triggers enhancement of low-frequency Cu spin fluctuations inhomogeneously; a growing fraction of  $^{139}\text{La}$  sites is affected by enhanced low-frequency spin fluctuations toward the eventual magnetic order, whereas a diminishing fraction continues to exhibit a behavior analogous to the optimally superconducting phase even below  $T_{\text{charge}}$ . These  $^{139}\text{La}$  NMR results corroborate our recent  $^{63}\text{Cu}$  NMR observation that a very broad, anomalous winglike signal gradually emerges below  $T_{\text{charge}}$ , whereas the normally behaving, narrower main peak is gradually wiped out [T. Imai *et al.*, *Phys. Rev. B* **96**, 224508 (2017)]. Furthermore, we show that the enhancement of low-energy spin excitations in the low-temperature regime below  $T_{\text{spin}}^{\text{neutron}} (\simeq T_c)$  depends strongly on the magnitude and orientation of the applied magnetic field.

DOI: [10.1103/PhysRevB.97.064511](https://doi.org/10.1103/PhysRevB.97.064511)**I. INTRODUCTION**

NMR probes the local electronic properties of solids via the hyperfine interactions between the observed nuclear spins and surrounding electrons. If the magnetic hyperfine interactions at a given atomic site are too strong, the NMR linewidth and relaxation rates usually undergo tremendous enhancement as one approaches magnetic instabilities from higher temperatures [1,2]. For example,  $^{63}\text{Cu}$  NMR and NQR (nuclear quadrupole resonance) linewidth and relaxation rates grow exponentially in the paramagnetic state of undoped  $\text{La}_2\text{CuO}_4$  due to the exponential growth of the spin-spin correlation length  $\xi$  [3,4]. Accordingly, detection of the paramagnetic  $^{63}\text{Cu}$  NMR and NQR signals becomes difficult below  $\sim 400$  K, nearly 100 K above the three-dimensional Néel transition at  $T_N \simeq 325$  K. This is also the fundamental reason behind the gradual disappearance of  $^{63}\text{Cu}$  NMR signals in the charge ordered state of  $\text{La}_2\text{CuO}_4$ -based cuprates near the doping concentration

around  $x \sim 1/8$ , because a growing volume fraction of  $\text{CuO}_2$  planes have divergently strong spin correlations [5–7].

In  $\text{La}_2\text{CuO}_4$ , the magnetic hyperfine interactions with Cu electron spins are two orders of magnitude weaker at the  $^{139}\text{La}$  (nuclear spin  $I = 7/2$  with the nuclear gyromagnetic ratio of  $\gamma_n/2\pi = 6.01$  MHz/T) sites than at  $^{63}\text{Cu}$  sites: the static hyperfine field  $B_N$  arising from Cu spins ordered in a staggered configuration is  $B_N \simeq 0.09$  T at  $^{139}\text{La}$  sites [8], whereas  $B_N \simeq 7.9$  T at  $^{63}\text{Cu}$  sites [9], both pointing along the diagonal direction within the  $\text{CuO}_2$  plane. Such a modest hyperfine coupling limits the growth of the  $^{139}\text{La}$  NMR linewidth and relaxation rates, and hence  $^{139}\text{La}$  NMR signals are always observable both above and below  $T_N$  [8]. Accordingly,  $^{139}\text{La}$  NMR is an effective probe of magnetic instabilities of the  $\text{CuO}_2$  planes in the  $\text{La}_2\text{CuO}_4$ -based superconductors, and played a crucial role in the early days of research into high-temperature superconductivity by establishing the magnetic phase diagram [10–12].

$^{139}\text{La}$  NMR was also used extensively to probe the stripe phase [13,14] of the superconducting  $\text{La}_{1.885}\text{Sr}_{0.115}\text{CuO}_4$  ( $T_c \simeq 30$  K) and related cuprates from early days [6,15–21], but the jumble of  $^{139}\text{La}$  NMR data acquired for different samples with different measurement conditions did not lead to a coherent physical picture for several reasons: First and foremost, many of the earlier  $^{139}\text{La}$  NMR experiments in  $\text{La}_{1.885}\text{Sr}_{0.115}\text{CuO}_4$  were limited to low-temperature regions without realizing that a charge order transition was lurking at as high as  $T_{\text{charge}} \simeq 80$  K [22–24]. Second, the lack of single crystals in the early days forced researchers to conduct powder NMR or zero field NQR, and hence only limited information was obtained. Third, as we discussed in great detail in the context of  $^{139}\text{La}$  NQR data for the charge and spin ordered  $\text{La}_{1.875}\text{Ba}_{0.125}\text{CuO}_4$  and  $\text{La}_{1.68}\text{Eu}_{0.2}\text{Sr}_{0.12}\text{CuO}_4$  [6], the glassy nature of spin ordering complicates the interpretation of the NMR data, because the apparent spin ordering temperature depends on the measurement time scales.

For example, in the prototypical stripe ordered materials such as  $\text{La}_{1.48}\text{Nd}_{0.4}\text{Sr}_{0.12}\text{CuO}_4$ ,  $\text{La}_{1.68}\text{Eu}_{0.2}\text{Sr}_{0.12}\text{CuO}_4$  and  $\text{La}_{1.88}\text{Ba}_{0.12}\text{CuO}_4$  with the low-temperature tetragonal (LTT) structure, elastic neutron scattering detects magnetic Bragg peaks at as high as  $T_{\text{spin}}^{\text{neutron}} \simeq 50$  K [13,25], because of the extremely fast measurement time scales ( $\sim 10^{-11}$  s) related to the integral taken over a small but finite energy transfer. On the other hand, muon spin rotation ( $\mu\text{SR}$ ) measurements, conducted in zero applied magnetic field, require a hyperfine magnetic field to be static over the duration of  $\sim 0.1$   $\mu\text{s}$  to detect the Larmor precessions in a magnetically ordered state, and a spin stripe order appears to occur only below  $T_{\text{spin}}^{\mu\text{SR}} \simeq 35$  K [14,26,27]. The apparent discrepancy arises, simply because fluctuations of Cu moments continue to slow down gradually below  $T_{\text{spin}}^{\text{neutron}}$  rather than suddenly becoming completely static. Our  $^{139}\text{La}$  NQR measurements of the nuclear spin  $I_z = \pm 3/2$  to  $\pm 1/2$  transition at  $\sim 6$  MHz registered the onset of line broadening due to a static  $B_N$  at even lower temperatures,  $\sim 20$  K [6]. This is because the NMR measurement time scale depends on the NMR frequency and the separation time  $\tau$  between the  $90^\circ$  and  $180^\circ$  radio-frequency pulses, and the latter is generally several  $\mu\text{s}$  or longer.

In this paper, we report high-precision  $^{139}\text{La}$  NMR measurements on a  $\text{La}_{1.885}\text{Sr}_{0.115}\text{CuO}_4$  single crystal. We independently verified the gradual onset of charge order transition at  $T_{\text{charge}} \simeq 80$  K by x-ray scattering measurements conducted at the SLAC [24]. We definitively identify the  $^{139}\text{La}$  NMR signatures of charge order transition at  $T_{\text{charge}} \simeq 80$  K, the onset of the three-dimensional spin order at  $T_{\text{spin}}^{\text{neutron}} \simeq 30$  K detected at the very fast time scale of elastic neutron-scattering measurements, and the onset of spin freezing at the slower time scale of  $\mu\text{SR}$  measurements at  $T_{\text{spin}}^{\mu\text{SR}} \simeq 15$ – $20$  K. We unequivocally demonstrate that charge order at  $T_{\text{charge}} \simeq 80$  K turns on inhomogeneous growth of low-frequency spin fluctuations, in agreement with our earlier conclusions [5–7]. On the other hand, since the amplitude of the charge density modulation is extremely small in the charge ordered state of  $\text{La}_{1.885}\text{Sr}_{0.115}\text{CuO}_4$ , as is evidenced by the difficulties faced by scatterers to detect Bragg peaks, we found no concrete evidence for a change in the electric-field gradient (EFG). Contrary to the presumption made by many authors, however, charge

order in  $\text{La}_{1.885}\text{Sr}_{0.115}\text{CuO}_4$  sets in very inhomogeneously in space, and a certain volume fraction of the  $\text{CuO}_2$  plane is not significantly affected by charge order even below  $T_{\text{charge}}$ ; such a volume fraction gradually diminishes with decreasing temperature. Furthermore, we show that  $B_{\text{ext}}$  applied normal to the  $\text{CuO}_2$  planes enhances the low-frequency spin fluctuations below  $T_{\text{spin}}^{\text{neutron}} (\simeq T_c)$ .

## II. EXPERIMENT

We used a single crystal of  $\text{La}_{1.885}\text{Sr}_{0.115}\text{CuO}_4$  grown at Tohoku with the traveling solvent floating zone techniques. The approximate dimensions of the crystal are  $2.5$  mm  $\times$   $2.5$  mm  $\times$   $1$  mm, and the long edges are parallel with the Cu-O-Cu bond direction. Magnetic susceptibility measurements using a superconducting quantum interference device (SQUID) showed a sharp bulk superconducting transition at  $T_c = 30$  K. We used an analogous specimen cut from the same boule of the present crystal for high precision x-ray-diffraction experiments at the SLAC, and detected a gradual onset of charge order below  $T_{\text{charge}} \simeq 80$  K [24]. A similar crystal of the same composition, also grown at Tohoku, was previously shown to exhibit an onset of static spin order at  $T_{\text{spin}}^{\text{neutron}} \simeq T_c \simeq 30$  K [28] at the neutron time scale and  $T_{\text{spin}}^{\mu\text{SR}} \simeq 20$  K [29] at the  $\mu\text{SR}$  time scale.

We conducted all the NMR measurements at McMaster based on standard pulsed NMR techniques using a state-of-the-art NMR spectrometer built around the Redstone NMR console acquired from Tecmag Inc. For the field geometry of  $B_{\text{ext}} \parallel ab$  plane, we utilized an aforementioned longer edge of the crystal as a guide for the alignment, and hence the external magnetic field  $B_{\text{ext}}$  is applied along the Cu-O-Cu bond direction.

We recently used the same piece of crystal for systematic  $^{63}\text{Cu}$  NMR measurements above and below  $T_{\text{charge}}$  for a wide range of NMR pulse separation time from  $\tau = 2$   $\mu\text{s}$  to  $30$   $\mu\text{s}$  [7]. We demonstrated that a relatively narrow central peak with properties analogous to the optimally superconducting  $\text{La}_{1.85}\text{Sr}_{0.15}\text{CuO}_4$  is gradually wiped out below  $T_{\text{charge}}$ , and the missing spectral weight is transferred to an extremely broad, winglike NMR signal; the latter can be detected only with very short  $\tau \lesssim 4$   $\mu\text{s}$ , and exhibits signatures of strongly enhanced spin correlations in the broad line shape and fast relaxation rates  $1/T_1$  and  $1/T_2$  [7].

## III. RESULTS AND DISCUSSIONS

### A. $^{139}\text{La}$ NMR linewidth $\Delta f$

In Fig. 1(a), we summarize  $^{139}\text{La}$  NMR line shapes observed for the nuclear spin  $I_z = +1/2$  to  $-1/2$  central transition in an external magnetic field  $B_{\text{ext}} = 9$  T applied along the crystal  $c$  axis. We also summarize the peak frequency  $f_o$  and the half width at half maximum (HWHM) of the line shape  $\Delta f$  in Fig. 2. For this field geometry, the  $^{139}\text{La}$  NMR line shape above the high temperature tetragonal (HTT) to low temperature orthorhombic (LTO) structural transition temperature at  $T_{\text{HTT-LTO}} \simeq 255$  K is so sharp that one can even use  $\Delta f$  to make fine adjustment for the alignment of the crystal [30,31]. This is because the  $\text{CuO}_6$  octahedra point straight up along the  $c$  axis, and hence the main principal axis of the electric-field gradient (EFG) tensor is parallel with  $B_{\text{ext}}$ , resulting in a null second-order quadrupole shift  $\Delta\nu_Q^{(2)}$  of  $f_o$ . The overall line

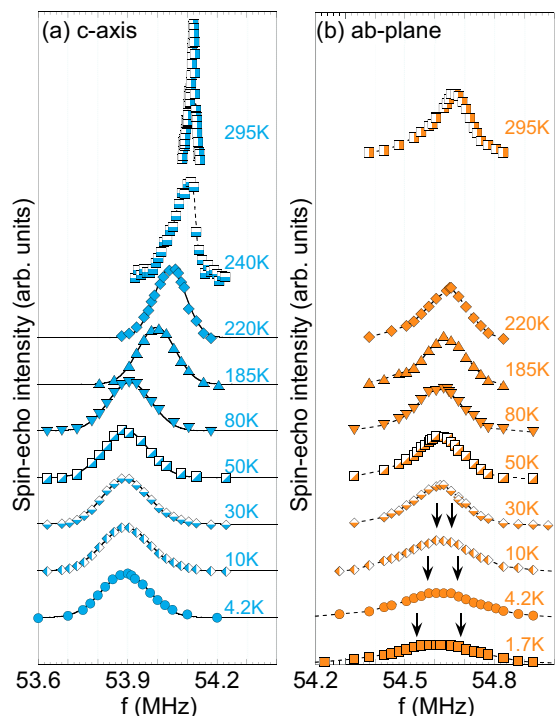


FIG. 1. (a) Representative <sup>139</sup>La NMR line shapes measured with a single crystal in  $B_{\text{ext}} = 9$  T applied along (a) the  $c$  axis and (b) the Cu-O-Cu bond direction within the  $ab$  plane. For clarity, the vertical origin is shifted at different temperatures. The solid curves through the  $c$  axis results at 220 K and below are the best Gaussian fits, whereas the dashed lines through all other asymmetrical line shapes are a guide for the eyes. Notice that the line shape continues to broaden even below  $T_{\text{spin}}^{\text{neutron}} = 30$  K for the  $ab$  plane, and the relatively sharp peak gives way to a wider flat-topped peak with two shoulders below  $\sim 10$  K, as marked by two arrows. Note that the shoulders are hardly observable even at  $\sim 10$  K ( $\ll T_{\text{spin}}^{\text{neutron}}$ ).

shape is asymmetric near 295 K due to the disorder caused by  $\text{Sr}^{2+}$  substitution, but narrow enough to be captured by the fast Fourier transform (FFT) of the spin-echo envelope down to 240 K. The half width is as narrow as  $\Delta f \simeq 6$  kHz at 295 K.

We found that the line shape for the  $B_{\text{ext}}||c$  axis is still somewhat asymmetrical at 220 K, but becomes almost perfect Gaussian at 180 K and below, as shown by solid curves through the line shapes in Fig. 1(a). Therefore, our results of  $\Delta f$  in Fig. 2(b) have a very high precision below 180 K, the critically important temperature range of our concern in this study. To maintain the consistency with  $\Delta f$  for the symmetrical line shapes observed below 180 K, we plot  $\Delta f$  estimated from the narrower side of the asymmetric line shape above 220 K.

As we cross  $T_{\text{HTT-LTO}} \simeq 250$  K into the LTO structure, the  $\text{CuO}_6$  octahedra begin to rotate alternately toward the diagonal direction of the  $\text{CuO}_2$  square lattice [32]. This results in a finite and temperature-dependent  $\Delta v_Q^{(2)} \propto v_Q^2/\gamma_n B_{\text{ext}}$  even for  $B_{\text{ext}}||c$ , where the nuclear quadrupole frequency at the <sup>139</sup>La sites is  $v_Q \sim 5.5$  MHz. Therefore, the peak frequency  $f_0$  shifts lower, as summarized in Fig. 2(a). Since both the rotation angle and  $v_Q$  have a distribution due to the disorder caused by  $\text{Sr}^{2+}$  substitution,  $\Delta f$  is strongly enhanced by the lattice effects below  $T_{\text{HTT-LTO}}$ , as readily seen in Figs. 1(a) and 2(b).

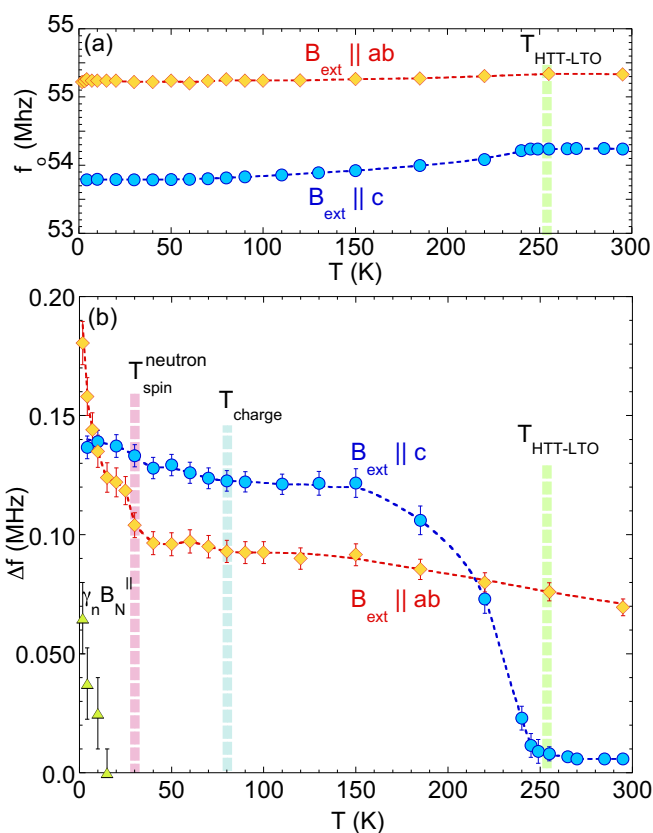


FIG. 2. (a) Temperature dependence of the <sup>139</sup>La NMR peak frequency  $f_0$ . (b) The HWHM of the <sup>139</sup>La NMR line shape,  $\Delta f$ . Dashed curves are a guide for eyes. Also shown (triangles) are  $\gamma_n B_N^{\parallel}$ , a half of the split between the two shoulders observed in the  $ab$ -plane line shapes below  $\sim 10$  K in Fig. 1(b), where  $B_N^{\parallel}$  is the projection of  $\vec{B}_N$  along the direction of the external magnetic field  $B_{\text{ext}}$ .

Let us turn our attention to the magnetic-field geometry of  $B_{\text{ext}}||ab$  plane. As shown in Fig. 1(b), the line shape is always asymmetric and already broad at 295 K, because  $\Delta v_Q^{(2)}$  is sizable for this geometry even in the HTT structure. With decreasing temperature, the NMR line is further broadened by a wide distribution of the rotation angle of the  $\text{CuO}_6$  octahedra.

For both the  $B_{\text{ext}}||c$ -axis and  $B_{\text{ext}}||ab$ -plane geometries,  $\Delta f$  saturates below  $\sim 150$  K. We confirmed from the measurements at 4.5 T that  $\Delta f$  above  $T_{\text{charge}}$  is inversely proportional to  $B_{\text{ext}}$  within experimental uncertainties. This means that  $\Delta f$  is dominated by the structural effects through the distribution of the EFG, because  $\Delta v_Q^{(2)} \propto 1/B_{\text{ext}}$ .

As noted above, owing to the nearly perfect Gaussian line shapes, our estimation of  $\Delta f$  for  $B_{\text{ext}}||c$  is of very high accuracy below 180 K. At  $T_{\text{charge}} \simeq 80$  K,  $\Delta f$  begins to show a subtle but clear sign of broadening again. Asymmetrical line shapes make determination of  $\Delta f$  with equally high precision more difficult for  $B_{\text{ext}}||ab$ , but  $\Delta f$  also grows by a somewhat smaller amount from  $T_{\text{charge}}$  to  $\sim 50$  K. We confirmed that the increase of  $\Delta f$  below  $T_{\text{charge}}$  is suppressed by a factor of  $\sim 2$  in 4.5 T. We also confirmed that the splitting  $v_Q$  between the  $I_z = +1/2$  to  $-1/2$  central peak and the  $I_z = \pm 1/2$  to  $\pm 3/2$  satellite peaks hardly changes between  $T_{\text{charge}}$  and 30 K, and the width of the latter remains unchanged across  $T_{\text{charge}}$ . Accordingly, the observed line broadening in the charge ordered state is paramagnetic

in origin, rather than the consequence of nuclear quadrupole effects. This implies that charge density modulation is *not* the direct cause of the broadening of  $\Delta f$  below  $T_{\text{charge}}$ , presumably because the amplitude of the charge density modulation is very small. Instead, enhanced spin correlations triggered by charge order are the indirect cause of the line broadening observed below  $T_{\text{charge}}$ . These findings are consistent with the strong paramagnetic  $^{63}\text{Cu}$  NMR line broadening we recently reported below  $T_{\text{charge}}$  for  $\tau \sim 2 \mu\text{s}$ . [7].

Although almost within experimental uncertainties,  $\Delta f$  seems to reach a plateau below  $\sim 50$  K for both field geometries, before additional line broadening sets in slightly above  $T_{\text{spin}}^{\text{neutron}} \simeq 30$  K. Again, the latter signals additional enhancement of antiferromagnetic spin correlations immediately before three-dimensional spin order begins at  $T_{\text{spin}}^{\text{neutron}}$ .

$\Delta f$  reaches another plateau at  $\sim 20$  K for both  $B_{\text{ext}}||c$  and  $B_{\text{ext}}||ab$  geometries, followed by strong enhancement only for  $B_{\text{ext}}||ab$  below  $T_{\text{spin}}^{\mu\text{SR}} \simeq 15\text{--}20$  K, where earlier  $\mu\text{SR}$  measurements showed that muons begin to exhibit Larmor precession about a static hyperfine magnetic field [14,29]. Below  $\sim 10$  K, shoulders develop in the line shapes as shown in Fig. 1(b), which we attribute to the emergence of a static hyperfine magnetic field  $\vec{B}_N$  at the  $^{139}\text{La}$  sites in the NMR measurement time scale. In what follows, we denote the projection of  $\vec{B}_N$  along the direction of  $\vec{B}_{\text{ext}}$  as  $B_N^||$ . Depending on the orientation of  $\vec{B}_N$  with respect to  $\vec{B}_{\text{ext}}$ , the static field  $B_N^||$  either enhances or suppresses the total magnetic field  $B_{\text{ext}} \pm B_N^||$  seen by each  $^{139}\text{La}$  nuclear spin, resulting in the upper and lower shoulder in the line shape, respectively. The temperature dependence of  $\gamma_n B_N^||$  summarized in Fig. 2(b) therefore reflects that of the magnitude of the statically ordered Cu moments in the NMR measurement time scale. The slow growth of  $B_N$  observed below  $\sim 10$  K in the present case is in contrast with our earlier finding that  $B_N$  quickly saturates in the low-temperature tetragonal (LTT) structure of  $\text{La}_{1.875}\text{Ba}_{0.125}\text{CuO}_4$  and  $\text{La}_{1.68}\text{Eu}_{0.2}\text{Sr}_{0.12}\text{CuO}_4$  below  $\sim 5$  and  $\sim 10$  K, respectively [6]. We also recall that a transverse magnetic field applied along the  $\text{CuO}_2$  planes has been shown to induce a spin-flop transition above  $\sim 5$  T in  $\text{La}_{1.885}\text{Sr}_{0.115}\text{CuO}_4$  [33,34] and above  $\sim 7$  T in  $\text{La}_{1.875}\text{Ba}_{0.125}\text{CuO}_4$  [20]. Due to the extremely weak NMR signal intensity below  $T_c$  for a single-crystal sample in the field geometry of  $B_{\text{ext}}||ab$ , the details of the spin-flop transition is beyond the scope of the present work.

We note that the magnitude of  $B_N^||$  has a large distribution stretching down to zero, and hence the  $^{139}\text{La}$  NMR line does not completely split even at 1.7 K. We measured the line shape at 1.7 K in Fig. 1(b) by repeating the spin-echo pulse sequence every  $t_{\text{rep}} = 23$  ms to saturate the slower component. The central part of the peak with longer  $T_1$  grows if we allow the nuclear spins to fully recover by using longer values of  $t_{\text{rep}}$ , resulting in somewhat obscured shoulders. The existence of  $^{139}\text{La}$  sites with  $B_N^|| \simeq 0$  observed here is consistent with an earlier report that Zeeman perturbed  $^{139}\text{La}$  NQR line does not split completely and just broadens [16]. These results are different from a sinusoidally modulating  $\vec{B}_N$  expected for a homogeneous incommensurate spin-density-wave state throughout the entire volume of the sample [35].  $\mu\text{SR}$  measurements also showed that  $\sim 80\%$  of the volume fraction of the  $\text{CuO}_2$  planes remains paramagnetic even at the base

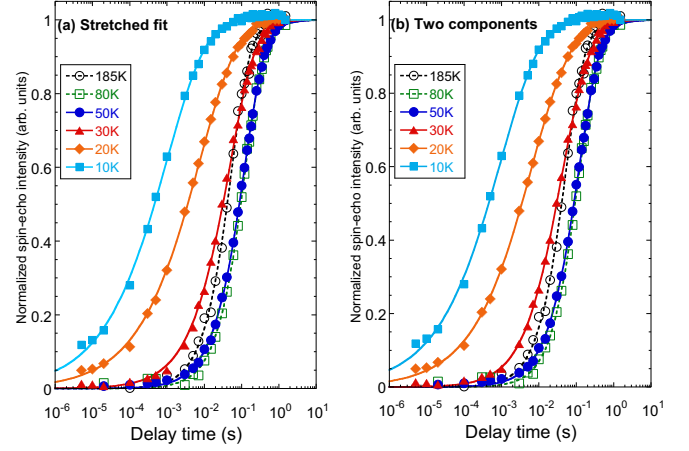


FIG. 3. (a) Representative spin-echo recovery curves  $M(t)$  after an inversion pulse. At  $T_{\text{charge}}$  and above, a free parameter fit with Eq. (2) leads to  $\beta = 1$  within experimental uncertainties (dashed curves). In the charge ordered state, a growing distribution  $1/T_1$  results in  $\beta < 1$  (solid curves). See Fig. 4(b) for the temperature dependence of  $\beta$ . (b) Two component fits with Eq. (3), with fast  $1/T_1^{\text{fast}}$  and slow  $1/T_1^{\text{slow}}$  components.

temperature, in which muons do not exhibit Larmor precession [29]. Therefore, we should indeed expect that as much as  $\sim 80\%$  of  $^{139}\text{La}$  sites might continue to see  $B_N^|| \sim 0$  at 1.7 K.

## B. Volume averaged behavior of low-frequency spin dynamics below $T_{\text{charge}}$

In order to investigate the influence of charge and spin order on Cu spin dynamics, we measured the nuclear-spin-lattice relaxation rate  $1/T_1$  at the central peak of the  $^{139}\text{La}$  sites. In the case of  $^{63}\text{Cu}$  and  $^{17}\text{O}$  NMR experiments, one can probe the different parts of the  $\text{CuO}_2$  planes with a different local hole concentration  $x_{\text{local}}$  by measuring  $1/T_1$  at a different frequency within a single NMR peak [31,36]. In the present case,  $^{139}\text{La}$  NMR signals from all different environments are superposed in a single peak, and hence we need to pay careful attention to the volume averaged nature of the  $^{139}\text{La}$   $1/T_1$  results when we interpret their implications.

Quite generally,  $1/T_1$  probes the Fourier component at the NMR frequency  $f_o (= \omega_o/2\pi)$  of the fluctuating hyperfine magnetic fields,

$$\frac{1}{T_1} = \frac{1}{2\hbar^2} \int_{-\infty}^{+\infty} \Sigma_{\alpha} \langle h_{\alpha}(\tau) h_{\alpha}(0) \rangle e^{-i\omega_o\tau} d\tau, \quad (1)$$

where the summation for  $\alpha$  is over two directions that are orthogonal to the quantization axis of nuclear spins set by  $B_{\text{ext}}$ , and  $h_{\alpha}$  represents the time-dependent fluctuating hyperfine magnetic field along the  $\alpha$  axis [1]. If we apply  $B_{\text{ext}}||c$  to measure  $1/T_1$ , the quantization axis is along the  $c$  axis, and hence  $\alpha = a$  or  $b$ . That is,  $1/T_1$  measured in  $B_{\text{ext}}||c$  probes the fluctuating hyperfine fields from Cu spins within the  $\text{CuO}_2$  planes, while  $1/T_1$  measured in  $B_{\text{ext}}||ab$  probes the fluctuations along both the  $c$  and  $ab$  planes.

In Fig. 3(a), we summarize representative results of the spin-echo recovery curve  $M(t)$  after an inversion pulse in an external magnetic field 9 T applied along the  $c$  axis. The solid curves represent the best fit with the appropriate fitting function

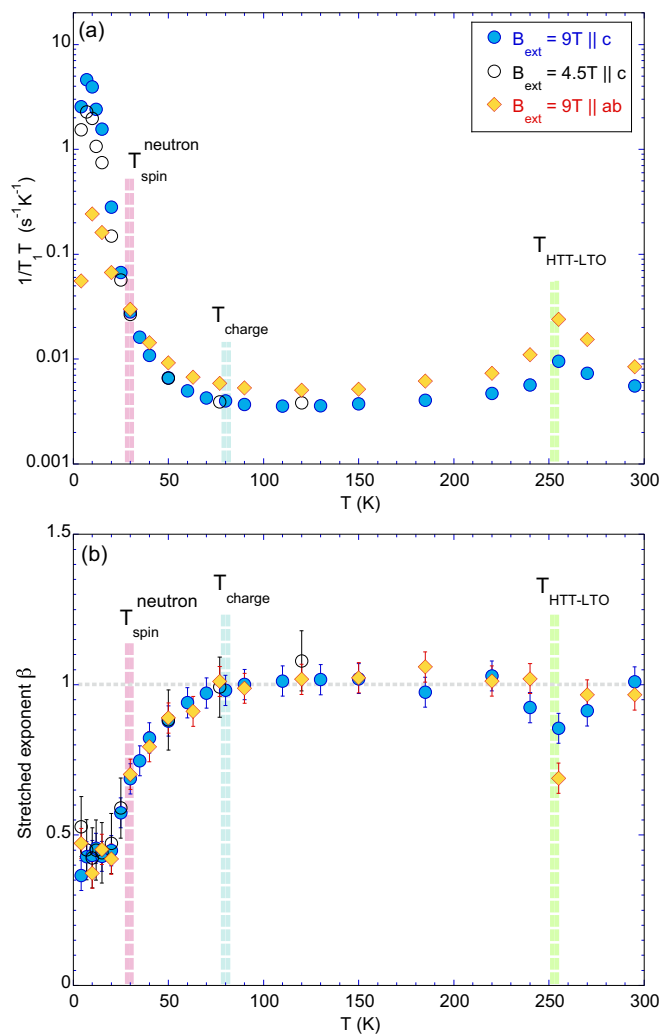


FIG. 4. (a) Temperature dependence of  $1/T_1T$  deduced from the best fit with Eq. (2), with a phenomenological stretched exponent  $\beta$  measured in  $B_{\text{ext}} = 9\text{ T}$  and  $4.5\text{ T}$  applied along the  $c$  axis or  $ab$  planes. (b) Temperature dependence of the stretched exponent  $\beta$ .

deduced for the magnetic transition ( $\Delta I_z = \pm 1$ ),

$$M(t) = A - B \left[ \sum_i p_i e^{-(q_i t / T_1)^\beta} \right], \quad (2)$$

where  $A$  and  $B$  are fitting parameters for the saturated and inverted signal intensity, respectively, and the coefficients  $(p_i, q_i)$  are theoretically calculated for each relevant normal mode [37,38]. For clarity, we present the normalized  $M(t)$  data in Fig. 3(a), so that it appears to be  $A = B = 1$  at all temperatures.  $\beta$  is an additional phenomenological parameter to enable the fit when the relaxation rate  $1/T_1$  has a distribution. If the relaxation process is purely magnetic and has no distribution, we expect  $\beta = 1$ . The stretched exponent  $\beta$  also enables us to fit  $M(t)$  phenomenologically, when the additional quadrupolar relaxation process with the  $\Delta I_z = \pm 2$  transitions contributes to the relaxation through the fluctuating EFG near the structural phase transition at  $T_{\text{HTT-LTO}}$  [37,39]. Separation of the quadrupole contribution to  $1/T_1$  is known to be a highly complicated process [39] and beyond the scope of the present work.

In Fig. 4(a), we summarize the temperature dependence of  $1/T_1$  divided by  $T$ ,  $1/T_1T$ , which reflects the wave vector  $\mathbf{q}$

integral within the first Brillouin zone of the imaginary part of the dynamical electron spin susceptibility  $\chi''(\mathbf{q}, f_o)$  at the NMR frequency  $f_o$  [40]. As explained in the Introduction, the hyperfine field  $B_N \sim 0.09\text{ T}$  is finite at the <sup>139</sup>La sites in the Néel state of  $\text{La}_2\text{CuO}_4$ . By definition, the wave-vector  $\mathbf{q}$  dependent hyperfine form factor  $A_{hf}(\mathbf{q})$  at the <sup>139</sup>La sites is related to  $B_N$  and the ordered Cu moment  $\mu_{\text{eff}}$  as  $B_N = |A_{hf}(\mathbf{q} = \mathbf{Q}_{AF})| \mu_{\text{eff}}$ , where  $\mathbf{Q}_{AF} = (\pi/a, \pi/a)$ . This means that  $A_{hf}(\mathbf{q} = \mathbf{Q}_{AF})$  is finite for the staggered wave vector  $\mathbf{Q}_{AF}$ , and hence antiferromagnetic spin fluctuations near  $\mathbf{q} \sim \mathbf{Q}$  can contribute to  $1/T_1$  measured at the <sup>139</sup>La sites.

Summarized in Fig. 4(b) is the temperature dependence of the corresponding stretched exponent  $\beta$ .  $1/T_1T$  shows very little temperature dependence down to  $T_{\text{charge}}$  except for a small cusp at  $T_{\text{HTT-LTO}}$  due to the enhanced slow fluctuations of the EFG associated with the lattice vibrations slowing down toward the structural transition [41]. The stretched exponent also deviates from  $\beta = 1$  near  $T_{\text{HTT-LTO}}$ , because the contribution of the additional quadrupole relaxation process invalidates the underlying assumption for the derivation of Eq. (2) based on purely magnetic transitions.

Once charge order sets in at  $T_{\text{charge}} \simeq 80\text{ K}$ , two qualitative changes take place. First, as shown in Fig. 4(a),  $1/T_1T$  begins to grow dramatically. Analogous enhancement of  $1/T_1T$  takes place below  $T_{\text{charge}}$  also at the planar <sup>17</sup>O sites [18,42]. These findings indicate that low-frequency Cu spin fluctuations averaged over the entire volume of the sample undergo a dramatic enhancement in the charge ordered state as temperature is lowered toward the onset of spin order at  $T_{\text{spin}}^{\text{neutron}} \simeq 30\text{ K}$ . We cannot entirely rule out a possibility from these data alone that quadrupole relaxation through fluctuating EFG is enhanced in the charge ordered state. However, we believe such a scenario is unlikely, because anomalous winglike signals emerge for <sup>63</sup>Cu NMR below  $T_{\text{charge}}$  with signatures of enhanced spin correlations [7]. Inelastic neutron-scattering experiments conducted with low-energy transfer also evidenced that low-frequency spin fluctuations are enhanced below  $T_{\text{charge}}$  [43].

Unlike the typical second-order magnetic phase transitions,  $1/T_1T$  does not diverge at  $T_{\text{spin}}^{\text{neutron}} \simeq 30\text{ K}$ . That is, critical slowing down of spin fluctuations does not lead to divergently large  $\chi''(\mathbf{Q}, f_o)$  at  $T_{\text{spin}}^{\text{neutron}}$  ( $\mathbf{Q}$  represents the ordering wave vector reported in Ref. [28]). Instead,  $1/T_1T$  keeps growing through  $T_{\text{spin}}^{\text{neutron}}$ , and exhibits a broad hump centered around  $\sim 8\text{ K}$ . In other words, spin ordering is indeed glassy, and the fluctuation time scale of Cu spins continue to slow down through  $T_{\text{spin}}^{\text{neutron}} \simeq 30\text{ K}$  and  $T_{\text{spin}}^{\mu SR} \simeq 20\text{ K}$ ; the average fluctuation frequency finally slows down to  $f_o$  only at  $\sim 8\text{ K}$ . This finding is consistent with the fact that the static hyperfine magnetic field  $B_N$  begins to grow gradually below  $T_{\text{spin}}^{\mu SR} \simeq 20\text{ K}$ .

The second change that manifests itself below  $T_{\text{charge}}$  is that the phenomenological stretched exponent begins to deviate from  $\beta = 1$ . This implies that the magnitude of  $1/T_1$  develops a broad range of distribution starting from  $T_{\text{charge}}$  toward the glassy spin ordering below  $T_{\text{spin}}^{\text{neutron}}$ .

### C. Two component behavior of low-frequency spin dynamics below $T_{\text{charge}}$

The phenomenological stretched fit with  $\beta < 1$  presented in Fig. 3(a) is satisfactory, but one needs to be cautious in

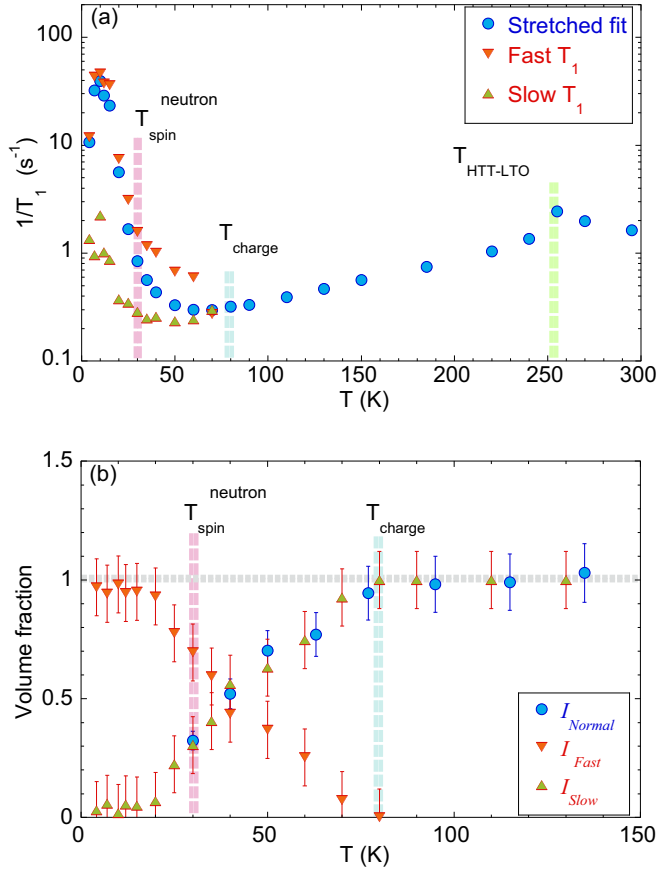


FIG. 5. (a) Comparison of  $1/T_1$  for  $B_{\text{ext}}||c$  deduced from the stretched fit with Eq. (2) (filled bullets); also shown in Fig. 4(a) in the form of  $1/T_1 T$  rather than  $1/T_1$  vs. two  $1/T_1^{\text{fast}}$  and  $1/T_1^{\text{slow}}$  values deduced from the two component fit with Eq. (3) (downward and upward triangles). (b) The fraction of  $^{139}\text{La}$  nuclear spins involved in the slower  $1/T_1$  component (upward triangles) show identical behavior as the spectral weight  $I_{\text{Normal}}$  of the narrower, normally behaving  $^{63}\text{Cu}$  NMR peak that seems almost oblivious to charge order and gradually wiped out below  $T_{\text{charge}}$  (adopted from Imai et al. [7]).

interpreting the resulting value of  $1/T_1$  because of its broad distribution. In fact, closer examination of the recovery curves observed at 30 and 185 K in Fig. 3(a) reveals that the former crosses the latter. That is, the distributed  $1/T_1$  at 30 K has both faster and slower components than a single valued  $1/T_1$  at 185 K. Our observation that a significant fraction of  $^{139}\text{La}$  nuclear spins still relax slowly below  $T_{\text{charge}}$  corroborates our recent finding that two different types of  $^{63}\text{Cu}$  NMR signals exist below  $T_{\text{charge}}$ , as mentioned at the end of Sec. II: the spectral weight  $I_{\text{Normal}}$  of the normally behaving narrow  $^{63}\text{Cu}$  NMR peak with slower  $1/T_1$  is gradually wiped out below  $T_{\text{charge}}$ , as reproduced from [7] in Fig. 5(b). The lost spectral weight is transferred to an anomalously broad, winglike  $^{63}\text{Cu}$  NMR signal which exhibits extremely fast  $1/T_1$ .

Since NMR is a local probe, if  $^{63}\text{Cu}$  NMR signals behave completely differently in a certain volume fraction,  $I_{\text{Normal}}$ , of the  $\text{CuO}_2$  planes,  $^{139}\text{La}$  NMR properties in the same volume would also be completely different. Accordingly, to maintain consistency between the  $^{139}\text{La}$  and  $^{63}\text{Cu}$  NMR results, it makes more sense to fit the recovery curves  $M(t)$  with two

components,

$$M(t) = A - B_1 \left[ \sum_i p_i e^{-(q_i t / T_1^{\text{fast}})^\beta} \right] - B_2 \left[ \sum_i p_i e^{-(q_i t / T_1^{\text{slow}})} \right]. \quad (3)$$

To achieve a good fit, we kept the stretched exponent  $\beta$  for the faster component  $1/T_1^{\text{fast}}$ , which arises from the segments of the  $\text{CuO}_2$  plane that yield the anomalous winglike  $^{63}\text{Cu}$  NMR signal with extremely fast  $1/T_1$ ; the slower component  $1/T_1^{\text{slow}}$  arises from the normally behaving volume in which  $^{63}\text{Cu}$  NMR properties seem almost oblivious to charge order even below  $T_{\text{charge}}$ . As shown in Fig. 3(b), the alternate fits with Eq. (3) are equally good.

We compare  $1/T_1^{\text{fast}}$  and  $1/T_1^{\text{slow}}$  in Fig. 5(a). The temperature dependence of  $\beta$  for the two-component fit is very similar to the result in Fig. 4(b). The behavior of  $1/T_1^{\text{fast}}$  is very similar to the volume averaged  $1/T_1$  estimated from the stretched fit using Eq. (2).  $1/T_1^{\text{slow}}$ , however, continues to decrease from  $T_{\text{charge}}$  down to the onset of spin order at  $T_{\text{spin}}^{\text{neutron}}$ . The observed temperature dependence of  $1/T_1^{\text{slow}}$  is qualitatively similar to the temperature dependence observed for the optimally superconducting  $\text{La}_{1.85}\text{Sr}_{0.15}\text{CuO}_4$  above its  $T_c = 38$  K [44,45].

Summarized in Fig. 5(b) is the volume fractions  $I_{\text{slow}} = B_2 / (B_1 + B_2)$  and  $I_{\text{fast}} = B_1 / (B_1 + B_2) = 1 - I_{\text{slow}}$  in which  $^{139}\text{La}$  nuclear spins relax with  $1/T_1^{\text{slow}}$  and  $1/T_1^{\text{fast}}$ , respectively. Quite remarkably,  $I_{\text{slow}}$  shows identical behavior as  $I_{\text{Normal}}$ , as expected, and gradually diminishes below  $T_{\text{charge}}$ . In contrast,  $I_{\text{fast}}$  grows from 0% at  $T_{\text{charge}}$  to  $\sim 70\%$  at  $T_{\text{spin}}^{\text{neutron}} \simeq T_c \simeq 30$  K, then to nearly 100%. The fact that  $I_{\text{fast}}$  reaches  $\sim 100\%$  at  $\sim 20$  K seems to suggest that, although the  $\mu\text{SR}$  data showed that  $\sim 80\%$  of the sample volume remains paramagnetic without a static hyperfine field [29], the entire volume of the  $\text{CuO}_2$  planes is in fact under the influence of enhanced spin fluctuations below  $\sim 20$  K. A potential caveat for this argument is that, since the superconducting shielding effects limit the NMR signal intensity below  $T_{\text{spin}}^{\text{neutron}} \simeq T_c \simeq 30$  K, we may be probing mostly the magnetic volume rather than the superconducting volume. But such a scenario seems highly unlikely in view of the fact that  $I_{\text{slow}}$  smoothly decreases through  $T_c$ .

#### D. Magnetic field effects on low-energy spin excitations

Earlier elastic neutron-scattering experiments found that application of a magnetic field normal to the  $\text{CuO}_2$  planes enhances the magnetic Bragg peak intensity arising from ordered spins below  $T_{\text{spin}}^{\text{neutron}}$  [46,47]. Such enhancement has been often attributed to the field-induced ordered moments within the superconducting vortex cores. In Fig. 4(a), we compare  $1/T_1 T$  measured in a magnetic field  $B_{\text{ext}} = 9$  T and 4.5 T applied along the  $c$  axis. The  $1/T_1 T$  results show no field dependence down to  $T_c \simeq T_{\text{spin}}^{\text{neutron}} \simeq 30$  K, where a substantial field dependence sets in. Interestingly,  $1/T_1 T$  reaches the maximum at the same temperature  $\sim 8$  K for 9 and 4.5 T, but the peak magnitude of  $1/T_1 T$  in 9 T is almost exactly twice larger than that observed in 4.5 T. Our finding is certainly consistent with the popular interpretation of the neutron data; when we apply twice stronger  $B_{\text{ext}}$ , the volume encompassed in the vortex core is doubled and hence its fast contribution to the volume averaged  $1/T_1 T$  also doubles. Note, however,

that such an argument is based on an assumption that both superconductivity and magnetic order take place uniformly within the CuO<sub>2</sub> planes, which may not be necessarily the case in La<sub>1.885</sub>Sr<sub>0.115</sub>CuO<sub>4</sub> according to local probe measurements reported here and elsewhere [5,7,29].

Another interesting aspect of our results in Fig. 4(a) is the anisotropy of  $1/T_1$ . The faster growth of  $1/T_1 T$  observed somewhat below  $T_{\text{charge}}$  for the  $B_{\text{ext}}||c$  than  $B_{\text{ext}}||ab$  geometry indicates that low-frequency spin fluctuations are more strongly enhanced within the  $ab$  plane. This is consistent with the fact that Cu spins eventually order along the CuO<sub>2</sub> planes in the low-temperature limit, as evidenced by the static hyperfine field  $B_N$  pointing along the CuO<sub>2</sub> planes.

Below  $\sim 15$  K, the anisotropy of  $1/T_1 T$  reaches a factor of  $\sim 10$ . An interesting possibility is that this is also caused by superconducting vortices. In  $B_{\text{ext}} = 9T||ab$ , the applied field is much smaller than the superconducting critical field  $B_{c2}$  owing to the layered structure, and the superconducting coherence length  $\xi$  is highly anisotropic ( $\xi_c \ll \xi_{ab}$ ). The area encompassed in the vortex core  $\sim \pi \xi_{ab} \xi_c$  for  $B_{\text{ext}}||ab$  is much smaller than  $\sim \pi \xi_{ab}^2$  for  $B_{\text{ext}}||c$ . Therefore, a much smaller peak value of  $1/T_1 T$  for  $B_{\text{ext}} = 9T||ab$  may be a consequence of the weaker influence of vortex cores penetrating through the CuO<sub>2</sub> planes. (The extremely small  $1/T_1 T \sim 0.5 \text{ s}^{-1} \text{ K}^{-1}$  observed at 4.2 K for  $B_{\text{ext}} = 9T||ab$  may be caused by the fact that we measured  $1/T_1$  at the center of the peak, where  $B_N^||$  is vanishingly small.)

#### IV. SUMMARY AND CONCLUSIONS

Three decades have passed since the discovery of high- $T_c$  superconductivity in La<sub>2</sub>CuO<sub>4</sub>-based materials, yet many fundamental issues remain unsolved. <sup>139</sup>La NMR in high magnetic fields is among the most straightforward NMR experiments for cuprates in terms of the technical requirements. Nonetheless, there was no comprehensive single-crystal <sup>139</sup>La NMR work on charge and spin ordered high- $T_c$  superconductor La<sub>1.885</sub>Sr<sub>0.115</sub>CuO<sub>4</sub> to date. Moreover, the physics of this composition has long been controversial, in part because glassiness of spin order and existence of superconductivity in spin ordered CuO<sub>2</sub> planes complicate the interpretation of experimental results. The controversy also stemmed from the fact that charge order Bragg peaks could not be detected by diffraction experiments until recently, and hence many researchers had continued to argue against the presence of charge order. We emphasize that we concluded the presence of charge order in La<sub>1.885</sub>Sr<sub>0.115</sub>CuO<sub>4</sub> with or without Eu codoping [5,6,48], La<sub>1.875</sub>Ba<sub>0.125</sub>CuO<sub>4</sub> [5,6,48], and La<sub>2</sub>CuO<sub>4+y</sub> [49] in as early as 1999, based on our findings that peculiar NMR anomalies associated with charge order of La<sub>1.48</sub>Nd<sub>0.4</sub>Sr<sub>0.12</sub>CuO<sub>4</sub> are shared by all of these materials.

To fill the knowledge gap and provide complementary information to the peculiar two-component behavior of <sup>63</sup>Cu NMR [5] recently confirmed below  $T_{\text{charge}}$  [7], we have conducted comprehensive single-crystal <sup>139</sup>La NMR experiments. From the high precision measurements of the linewidth  $\Delta f$  and spin-lattice relaxation rate  $1/T_1$ , we have identified the anomalies associated with charge order and glassy spin order, and cleared up the confusions from the past. Combined with the successful detection of charge order Bragg peaks in La<sub>1.885</sub>Sr<sub>0.115</sub>CuO<sub>4</sub>

[22–24] and related materials [25,50] in recent years, we believe that a clear-cut physical picture is finally emerging.

Perhaps the most significant message from our local probe study, with possibly far reaching implications, is that charge ordered CuO<sub>2</sub> planes in La<sub>1.885</sub>Sr<sub>0.115</sub>CuO<sub>4</sub> become extremely inhomogeneous, and have two distinct regions with contrasting characteristics: (a) normal regions with the volume fraction  $I_{\text{slow}} (\simeq I_{\text{Normal}}$  observed for <sup>63</sup>Cu NMR [7]), which are not affected significantly by charge order, and (b) charge ordered regions with continuously growing spin correlations from  $T_{\text{charge}}$  through  $T_{\text{spin}}^{\text{neutron}}$ . The <sup>139</sup>La and <sup>63</sup>Cu NMR properties in the normal regions are qualitatively similar to those observed for the optimally superconducting La<sub>1.85</sub>Sr<sub>0.15</sub>CuO<sub>4</sub>, but its volume fraction gradually decreases from 100% at  $T_{\text{charge}}$  to  $\sim 0\%$  at  $\sim 20$  K. It remains to be seen whether our finding is directly related to the nematicity expected for the charge ordered CuO<sub>2</sub> planes [51]. It is also worth noting that the difference in the ground state energy is very small between the uniform d-wave superconducting state (dSC) and a coexisting hole stripe-SDW-dSC state [52,53]. We emphasize that NMR is a local probe. In contrast, neutron and x-ray scattering measurements on charge and spin order phenomena are conducted in the  $\mathbf{q}$  space by integrating the scattering intensity from the entire volume of the sample, and hence probe only the volume averaged behavior of the CuO<sub>2</sub> planes.

We should note that our  $\Delta f$  results for  $B_{\text{ext}}||ab$  are similar to the pioneering powder <sup>139</sup>La NMR data reported by Goto *et al.* below 60 K [15,17,34]. They did not extend their  $\Delta f$  measurements to the crucial temperature region across  $T_{\text{charge}}$ , because their initial 1994 work preceded the discovery of charge order phenomenon in La<sub>1.48</sub>Nd<sub>0.4</sub>Sr<sub>0.12</sub>CuO<sub>4</sub> by Tranquada *et al.* in 1995 [13]. More recently, after we concluded that La<sub>1.885</sub>Sr<sub>0.115</sub>CuO<sub>4</sub> with or without Eu codoping also undergoes a charge order [5,6,18,48], the Grenoble group reported a limited set of <sup>139</sup>La single-crystal NMR data for La<sub>1.88</sub>Sr<sub>0.12</sub>CuO<sub>4</sub> in a tilted magnetic field up to 100 K [19]. Some parts of their results are similar to Goto's results and ours reported here and elsewhere [18]. The Grenoble paper as well as an earlier work on La<sub>1.65</sub>Eu<sub>0.2</sub>Sr<sub>0.15</sub>CuO<sub>4</sub> by the Los Alamos group [54], however, interpreted their NMR data based on a presumption that charge order is absent in the superconducting cuprates. Very recent <sup>139</sup>La NMR work on the charge ordered state realized in the LTT structure of La<sub>1.88</sub>Ba<sub>0.12</sub>CuO<sub>4</sub> with suppressed superconductivity [20] share many similarities with the present case, but there are two important dissimilarities: First, the magnetic correlations in La<sub>1.88</sub>Ba<sub>0.12</sub>CuO<sub>4</sub> grow very quickly below  $T_{\text{charge}} = 54$  K, and  $1/T_1$  seems to reach a plateau at  $T_{\text{spin}}^{\text{neutron}} = 40$  K. Second, application of a high magnetic field *suppresses*  $1/T_1$  in the spin ordered phase of La<sub>1.88</sub>Ba<sub>0.12</sub>CuO<sub>4</sub>, whereas a magnetic field *enhances*  $1/T_1$  in the present case.

*Note added.* We recently observed analogous <sup>139</sup>La NMR anomalies at  $\sim 60$  K for Sr concentration  $x = 0.10$  and  $0.13$ . Combined with the present result, the phase diagram exhibits a charge order dome peaked at  $x = 0.115$ .

#### ACKNOWLEDGMENTS

T.I. thanks T. M. Rice for helpful communications. The work at McMaster was financially supported by NSERC and

CIFAR. The work at Stanford was supported by US Department of Energy, Office of Science, Office of Basic Energy Sciences and Engineering Division under Grant No. DE-AC02-

76SF00515. The work at Tohoku was supported by Grant-in-Aid for Scientific Research (A) (Grant No. 16H02125), Japan.

- 
- [1] V. Jaccarino, *Nuclear Resonance in Antiferromagnets*, edited by G. T. Rado and H. Suhl, Vol. Magnetism IIA (Academic, New York, 1965).
- [2] P. Heller and G. B. Benedek, *Phys. Rev. Lett.* **8**, 428 (1962).
- [3] T. Imai, C. P. Slichter, K. Yoshimura, and K. Kosuge, *Phys. Rev. Lett.* **70**, 1002 (1993).
- [4] T. Imai, C. P. Slichter, K. Yoshimura, M. Katoh, and K. Kosuge, *Phys. Rev. Lett.* **71**, 1254 (1993).
- [5] A. W. Hunt, P. M. Singer, K. R. Thurber, and T. Imai, *Phys. Rev. Lett.* **82**, 4300 (1999).
- [6] A. W. Hunt, P. M. Singer, A. F. Cederström, and T. Imai, *Phys. Rev. B* **64**, 134525 (2001).
- [7] T. Imai, S. K. Takahashi, A. Arsenault, A. W. Acton, D. Lee, W. He, Y. S. Lee, and M. Fujita, *Phys. Rev. B* **96**, 224508 (2017).
- [8] H. Nishihara, H. Yasuoka, T. Shimizu, T. Tsuda, T. Imai, S. Sasaki, S. Kanbe, K. Kishio, K. Kitazawa, and K. Fueki, *J. Phys. Soc. Jpn.* **56**, 4559 (1987).
- [9] T. Tsuda, T. Shimizu, H. Yasuoka, K. Kishio, and K. Kitazawa, *J. Phys. Soc. Jpn.* **57**, 2908 (1988).
- [10] I. Wataneba, K. Kumagai, Y. Nakamura, T. Kimura, Y. Nakamichi, and H. Nakajima, *J. Phys. Soc. Jpn.* **56**, 3028 (1987).
- [11] Y. Kitaoka, K. Ishida, S. Hiramatsu, and K. Asayama, *J. Phys. Soc. Jpn.* **57**, 734 (1988).
- [12] F. C. Chou, F. Borsa, J. H. Cho, D. C. Johnston, A. Lascialfari, D. R. Torgeson, and J. Ziolo, *Phys. Rev. Lett.* **71**, 2323 (1993).
- [13] J. M. Tranquada, B. J. Sternlieb, J. D. Axe, Y. Nakamura, and S. Uchida, *Nature (London)* **375**, 561 (1995).
- [14] K. Kumagai, K. Kawano, I. Watanabe, K. Nishiyama, and K. Nagamine, *Hyperfine Interact.* **86**, 473 (1994).
- [15] T. Goto, S. Kazama, K. Miyagawa, and T. Fukase, *J. Phys. Soc. Jpn.* **63**, 3494 (1994).
- [16] S. Ohsugi, Y. Kitaoka, H. Yamanaka, K. Ishida, and K. Asayama, *J. Phys. Soc. Jpn.* **63**, 2057 (1994).
- [17] T. Goto, T. Suzuki, K. Chiba, T. Shinoda, M. Mori, and T. Fukase, *Physica B* **246**, 572 (1998).
- [18] T. Imai and K. Hirota (unpublished).
- [19] V. F. Mitrović, M.-H. Julien, C. de Vaulx, M. Horvatić, C. Berthier, T. Suzuki, and K. Yamada, *Phys. Rev. B* **78**, 014504 (2008).
- [20] S.-H. Baek, Y. Utz, M. Hücker, G. D. Gu, B. Büchner, and H.-J. Grafe, *Phys. Rev. B* **92**, 155144 (2015).
- [21] S.-H. Baek, A. Erb, and B. Büchner, *Phys. Rev. B* **96**, 094519 (2017).
- [22] T. P. Croft, C. Lester, M. S. Senn, A. Bombardi, and S. M. Hayden, *Phys. Rev. B* **89**, 224513 (2014).
- [23] V. Thampy, M. P. M. Dean, N. B. Christensen, L. Steinke, Z. Islam, M. Oda, M. Ido, N. Momono, S. B. Wilkins, and J. P. Hill, *Phys. Rev. B* **90**, 100510 (2014).
- [24] W. He, Y. S. Lee, and M. Fujita (unpublished).
- [25] M. Fujita, H. Goka, K. Yamada, J. M. Tranquada, and L. P. Regnault, *Phys. Rev. B* **70**, 104517 (2004).
- [26] G. M. Luke, L. P. Le, B. J. Sternlieb, W. D. Wu, Y. J. Uemura, J. H. Brewer, and Riseman, *Physica C* **185**, 1175 (1991).
- [27] B. Nachumi, Y. Fudamoto, A. Keren, K. M. Kojima, M. Larkin, G. M. Luke, J. Merrin, O. Tchernyshyov, Y. J. Uemura, N. Ichikawa, M. Goto, H. Takagi, S. Uchida, M. K. Crawford, E. M. McCarron, D. E. MacLaughlin, and R. H. Heffner, *Phys. Rev. B* **58**, 8760 (1998).
- [28] H. Kimura, K. Hirota, H. Matsushita, K. Yamada, Y. Endoh, S.-H. Lee, C. F. Majkrzak, R. Erwin, G. Shirane, M. Greven, Y. S. Lee, M. A. Kastner, and R. J. Birgeneau, *Phys. Rev. B* **59**, 6517 (1999).
- [29] A. T. Savici, Y. Fudamoto, I. M. Gat, T. Ito, M. I. Larkin, Y. J. Uemura, G. M. Luke, K. M. Kojima, Y. S. Lee, M. A. Kastner, R. J. Birgeneau, and K. Yamada, *Phys. Rev. B* **66**, 014524 (2002).
- [30] K. R. Thurber, A. W. Hunt, T. Imai, F. C. Chou, and Y. S. Lee, *Phys. Rev. Lett.* **79**, 171 (1997).
- [31] P. M. Singer, T. Imai, F. C. Chou, K. Hirota, M. Takaba, T. Kakeshita, H. Eisaki, and S. Uchida, *Phys. Rev. B* **72**, 014537 (2005).
- [32] B. Grande, H. K. Müller-Buschbaum, and M. Schweizer, *Z. Anorg. Allg. Chem.* **428**, 120 (1977).
- [33] T. Goto, K. Chiba, M. Mori, T. Suzuki, K. Seki, and T. Fukase, *J. Phys. Soc. Jpn.* **66**, 2870 (1997).
- [34] K. Chiba, T. Goto, M. Mori, T. Suzuki, K. Seki, and T. Fukase, *J. Low Temp. Phys.* **117**, 479 (1999).
- [35] F. L. Ning, M. Fu, D. A. Torchetti, T. Imai, A. S. Sefat, P. Cheng, B. Shen, and H.-H. Wen, *Phys. Rev. B* **89**, 214511 (2014).
- [36] P. M. Singer, A. W. Hunt, and T. Imai, *Phys. Rev. Lett.* **88**, 047602 (2002).
- [37] E. R. Andrew and D. P. Tunstall, *Proc. Royal Soc.* **78**, A1 (1960).
- [38] A. Narath, *Phys. Rev.* **162**, 320 (1967).
- [39] A. Suter, M. Mali, J. Roos, and D. Brinkmann, *J. Phys.: Condens. Matter* **10**, 5977 (1998).
- [40] T. Moriya, *J. Phys. Soc. Jpn.* **18**, 516 (1963).
- [41] R. J. Birgeneau, C. Y. Chen, D. R. Gabbe, H. P. Jenssen, M. A. Kastner, C. J. Peters, P. J. Picone, T. Thio, T. R. Thurston, H. L. Tuller, J. D. Axe, P. Böni, and G. Shirane, *Phys. Rev. Lett.* **59**, 1329 (1987).
- [42] T. Imai and K. Hirota, *J. Phys. Soc. Jpn.* **87**, 025004 (2018).
- [43] A. T. Rømer, J. Chang, N. B. Christensen, B. M. Andersen, K. Lefmann, L. Mähler, J. Gavilano, R. Gilardi, C. Niedermayer, H. M. Rønnow, A. Schneidewind, P. Link, M. Oda, M. Ido, N. Momono, and J. Mesot, *Phys. Rev. B* **87**, 144513 (2013).
- [44] T. Kobayashi, S. Wada, Y. Kitaoka, and K. Asayama, *J. Phys. Soc. Jpn.* **58**, 2262 (1989).
- [45] K. Yoshimura, T. Uemura, M. Kato, T. Shibata, K. Kosuge, T. Imai, and H. Yasuoka, *Springer Proc. Phys.* **60**, 405 (1992).
- [46] B. Lake, H. M. Ronnow, N. B. Christensen, G. Aeppli, K. Lefmann, D. F. McMorrow, P. Vorderwisch, P. Smeibid, N. Mangkorntong, T. Sasagawa, M. Nohara, H. Takagi, and T. E. Mason, *Nature (London)* **415**, 299 (2002).
- [47] B. Khaykovich, S. Wakimoto, R. J. Birgeneau, M. A. Kastner, Y. S. Lee, P. Smeibid, P. Vorderwisch, and K. Yamada, *Phys. Rev. B* **71**, 220508 (2005).



- [48] P. M. Singer, A. W. Hunt, A. F. Cederström, and T. Imai, *Phys. Rev. B* **60**, 15345 (1999).
- [49] T. Imai and Y. S. Lee, [arXiv:1712.09720](https://arxiv.org/abs/1712.09720).
- [50] J. Fink, V. Soltwisch, J. Geck, E. Schierle, E. Weschke, and B. Büchner, *Phys. Rev. B* **83**, 092503 (2011).
- [51] S. A. Kivelson, E. Fradkin, and V. J. Emery, *Nature (London)* **393**, 550 (1998).
- [52] A. Himeda, T. Kato, and M. Ogata, *Phys. Rev. Lett.* **88**, 117001 (2002).
- [53] P. Corboz, T. M. Rice, and M. Troyer, *Phys. Rev. Lett.* **113**, 046402 (2014).
- [54] N. J. Curro, P. C. Hammel, B. J. Suh, M. Hücker, B. Büchner, U. Ammerahl, and A. Revcolevschi, *Phys. Rev. Lett.* **85**, 642 (2000).